Light Metals 2012 *Edited by: Carlos E. Suarez*
TMS (The Minerals, Metals & Materials Society), 2012

Post Weld Heat Treatment of Friction Stir Welded AA2017

M.M.Z. Ahmed [1] * and B.P. Wynne [2]
[1] Department of Metallurgical and Materials Engineering, Faculty of Petroleum and Mining Engineering, Suez Canal University, Suez 43721,Egypt.
[2] Institute for Microstructural and Mechanical Processing Engineering: The University of Sheffield (IMMPETUS), Mappin Street, Sheffield S1 3JD, UK.
*Tel: (+2) 0623360252, email: mohamed_ahmed4@s-petrol.suez.edu.eg

Keywords: Friction Stir Welding, Post Weld Heat Treatment, Aluminum Alloy, Electron Back Scattering Diffraction

Abstract

In this study a friction stir welded AA2017 is post weld heat treated at 500 °C for holding time of 20, 40 and 60min then quenched in water and naturally aged. The effect of post weld heat treatment on the microstructure and hardness is investigated across the transverse cross section of the weld. Experimental results showed that the PWHT causes abnormal grain growth of the grain structure mainly near to the advancing side of the weld. The grain size increases with the increase of the holding time however the region near to the retreating side of the weld retained its fine grain structure. EBSD has been used to examine the microstructure and texture before and after PWHT. EBSD investigation showed that the grain growth is texture dependant as grain growth occurs in some grains of (B+C) texture component while in the adjacent grains of texture components B- does not occur.

Introduction

Friction stir welding of heat treatable aluminum alloys such as 2xxx [1-4], 6xxx [5, 6] and 7xxx [7, 8] results in a fine grain structure in the nugget region NG region [7, 9] and also in a softened region at the thermomechanically affected zone (TMAZ) and the heat affected zone (HAZ) [6, 9]. Post weld heat treatment (PWHT) represents the obvious option to recover the loss of strength across the weld zone. However, the high temperature experienced during solution treatment results in abnormal grain growth (AGG) in the NG [1-4]. Hassan et al [10] studied the stability of NG grain structure during solution treatment and reported that the NG grain structure is unstable during solution treatment mainly due to the very fine grain structure and the partial dissolution of second phase penning particles. This instability of grain structure attributed to the inhomogeneous deformation pattern during the friction stir processing of AA7075 by Charit and Mishra [8] and they found that having a certain combinations of tool rotation rate and traverse speed can eliminate the AGG. This also was noted before by Attallah and Salem[3] in an investigation to study the effect of FSW parameters on the AGG of FSWed AA2095 grain structure during PWHT and they reported that the tool rotation rate and traverse speed greatly affect the extent of AGG. According to the previous studies [3, 8] the AGG can be controlled initially via the control of the processing parameters; rotation rate and traverse speed. This is important to keep the fine grain structure in the same time with the recovery of strength via PWHT. A number of studies reported the usefulness of PWHT in the improvement of strength after FSW [1, 4, 5]. Chen et al[1] studied the effect of PWHT on the mechanical properties of FSWed AA2219 and found that the tensile strength of the heat treated joints increases with increasing solution treatment temperature. Elangovan and Balasubramanian [5] studied the effect of PWHT on the tensile properties of AA6061 and found that solution treatment followed by artificial aging is important to enhance tensile properties of FSWed AA6061. Also Aydin et al [4] investigated the effect of PWHT on the mechanical properties of FSWed AA2024-T4 and found that the T6 ageing treatment after welding is beneficial in enhancing the mechanical properties of the 2024-T4 joints. In this work the effect of solution treatment time on the hardness and microstructure of FSWed AA22017A has been investigated and also the dependence of the AGG on the crystallographic texture of the NG has been examined.

Experimental Work

Three sections of friction stir welded AA2017A plate of 20mm thickness were post weld heat treated by solution treatment at 500 °C for 20min, 40 min and 60min and then naturally aged for 55 days(details of FSW parameters and tool given elsewhere[11]) . The sections prepared according to the standard grinding and polishing and then etched using diluted Keller's reagent to reveal the microstructure. Optical macrograph for the whole sections has been made. Vickers hardness was measured with 5Kg load in a two dimensional grid with a 4mm spacing in order to construct a hardness map which could then be correlated with microstructure observations. A sample has been cut from the as welded and the 60min solution treated section for Electron Back Scattered Diffraction (EBSD) investigation. These samples were then mechanically polished and subsequently electropolished with a solution of 30% Nitric acid in methanol for 60 seconds at 14 V at -15 °C. A Sirion scanning electron microscope equipped with a Nordlys CCD camera controlled by HKL Channel 5 software has been used for EBSD data acquisition. For microstructure and texture analysis a 2μm step size used. The obtained data was then analyzed using HKL Channel 5 software.

Results and Discussion

Hardness Maps

After PWHT the sections were prepared for Vickers hardness measurement and hardness map distribution for each condition was constructed. Figure 1 shows the hardness map for the as FSWed section in (Figure 1 a) and after PWHT for 20min, 40min and 60min in (Figure 1 b, c and d) respectively. In the hardness map of the as FSWed material it can be observed that the hardness distribution follows the typical hardness distribution for the FSWed heat treatable aluminum alloys [6, 12-14] in which the hardness decreased in the HAZ and the TMAZ with the lowest hardness at the interface between TMAZ and HAZ. It can be observed also that the hardness in the NG region almost the same as that of the parent metal (about 170HV) mainly at the top part of the NG and slightly decreasing further down. The decrease in

hardness at the HAZ and TMAZ is mainly due to the coarsening and /or dissolution of the precipitation hardening phases [15] [8]. As it is already known that the NG is part from the TMAZ [16] which experiences both high temperature and high strain, those are enough to produce fine grain structure in the NG and not in the rest of TMAZ towards the HAZ [16]. The question rise now is the hardness increase in the NG due to the re-precipitation during the cooling cycle or due to natural aging after FSW? The hardness maps after PWHT may help answering this question.

The hardness map after PWHT for the solution treated specimen for 20 min shows a hardness range similar to that existing in the HAZ of the as welded section, which indicate that the PWHT scheme of 20min + natural aging was not enough to fully harden the alloy. Also after 40min still the hardness map quite similar to that after 20min. The hardness map after PWHT for 60min indicate a higher range of hardness but still does not reach the full hardening of the alloy. The results of hardness after the applied PWHT schemes clearly shows that natural aging for 55days after ST at 500 °C for up to 60min could not result in the full hardening that occurred in the NG after FSW only. This would suggest that the hardening that occurred in the NG region after FSW has been occurred during the cooling cycle after FSW. This hardening was enhanced by the existence of high strain that would induce precipitation during the cooling cycle. Strain induced precipitation is reported in many materials such as Ni base alloys [17], in steel [18] as well as aluminum alloys [19]. The presence of strain induced precipitation can explain the increase of hardness in the highly deformed region in the weld relative to that increase obtained by the normal heat treatment.

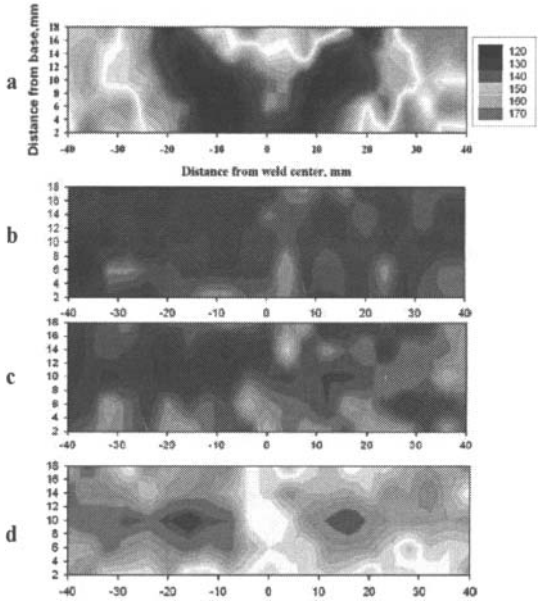

Figure 1. Vickers hardness maps a) as FS welded; b, c and d) After PWHT at 500°C for 20min, 40min and 60min respectively followed by natural aging for 55 days.

Optical Microstructure

Stitched optical micrographs of the whole NG region for the as FS welded section is illustrated in Figure 2. The NG region of the as FSWed section is dominated by very fine grain structure with some clear banding at the advancing side of the NG (detailed microstructure of this weld given elsewhere [11]). The stitched optical micrographs of the whole NG for the PWHTed sections are shown in Figure 3(a-c). It can be observed that after 20 min ST AGG occurred at the bottom of the NG and in a very thin layer at the top of the NG. Also some coarse grains were formed at the AS near the bottom of the NG mainly replacing some bands that observed in the as FSWed section. After 40min ST, the AGG extended in a wider area in the NG towards the AS replacing more bands that observed in the as FSWed section. Also some grain coarsening spread inside the NG can be observed mainly towards the AS. At the top surface coarsening occurred approximately in a thin layer similar to that observed after 20min ST. It can be observed that there is no significant change in the size of the coarse grains after 20 and 40min at the ST. Two main differences between 20 and 40min ST sections can be observed, first the grain coarsening that spread in a wider areas in the NG and second the appearance of the oxide line remainant (known as zigzag line [20, 21]) after 40min ST. However after 60min ST it can be seen that the coarse grains that formed at the bottom of the NG and near the AS after 20 and 40min have been greatly coarsened to the extent that only a few number of very large grains occupied approximately the same grain coarsening area. Figure 4 shows the optical micrographs after 20min ST (Figure 4.a) and after 60min in (Figure 4.b), which showing the progress of the AGG by increasing ST time. The grain coarsening only extended to small areas after 60min with the majority of the NG near the retreating side (RS) retaining their fine grain structure that formed after FSW. This implies that the heterogeneity in the deformation pattern exist within the NG of the same weld which resulted in the AGG in some areas and not in the others. This heterogeneity was observed before in the form of alternating bands of different texture components in the NG region [22, 23]. Fonda and Bingert [23] reported that the banding structure in the NG of FSWed AA2195 corresponds to a periodic textural variation between the B/-B component and a mixture of B/-B and C components of the simple shear texture. Also Ahmed et al [22] observed alternating bands between B and -B simple shear texture components across the NG of FSWed AA6082. The effect of this textural variation on the AGG was examined using EBSD and given the next section below.

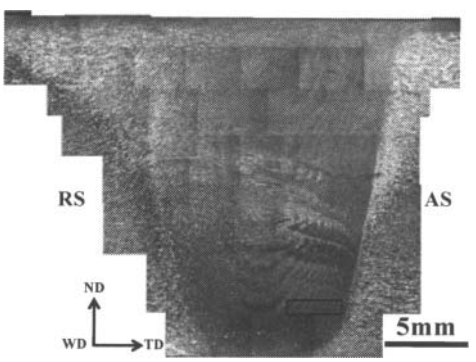

Figure 2 A stitched optical micrographs for the NG region of as FSWed AA2017.

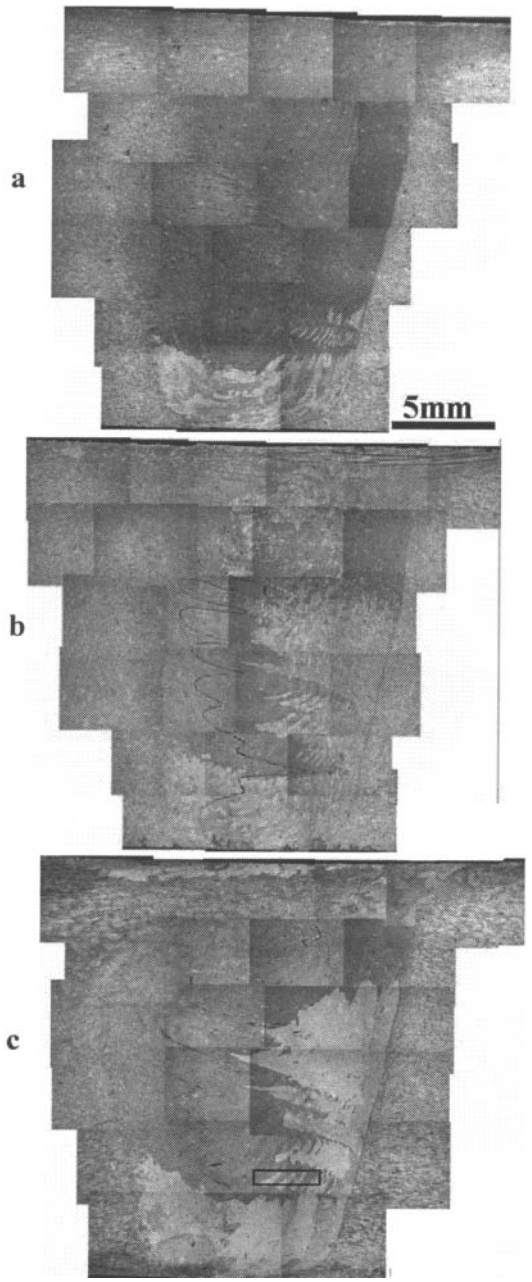

Figure 3, Stitched optical micrographs for the whole NG of the PWHTed sections at 500 °C for a) 20min, b)40min and c) 60min.

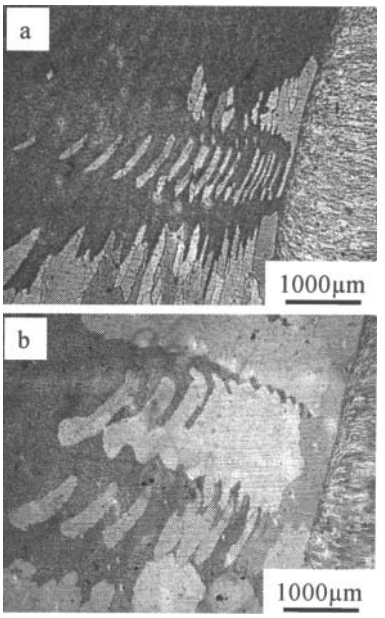

Figure 4 Optical micrographs showing the progress of the AGG by increasing ST time from 20min a) to 60 min b).

EBSD Microstructure and Texture

EBSD has been used to examine the microstructure and texture before and after PWHT and two EBSD maps have been acquired using 2μm step size. The first one acquired from the as FSWed section and the PWHTed section for 60 min approximately at the same position that indicated by rectangles in Figure 2 and Figure 3.c..

Figure 5a shows the orientation image map (OIM) of the raw EBSD data set acquired from the as FSWed section using inverse pole figure (IPF) colouring with respect to the ND of the weld. The map clearly shows alternating bands between near <110> (green) and near <111> (blue) grain orientation across the whole map. Figure 5b shows the texture component map for the data set shown in Figure 5a after relating the data set to the local shear reference frame according to the methodology described before [22]. The texture component map has highlighted the (red), (yellow) and C (blue) components with a 25° spread. From the texture component map it can be observed that these bands are between texture components (C+B) (Red + blue) and texture component $\overline{B}$ (yellow). The OIM acquired approximately at the same position from the 60min PWHTed section is illustrated in Figure 5c. It can be observed that the grain structure consists of the original fine grain structure that observed in the as FSWed map and some very large grains tilted at an angle from the ND and separated by bands of fine grains. By comparing the positions of the large grain with the texture component map it can be noticed that those large grains were formed in the bands that have (C+B) (Red + blue) texture components. This implies that the bands of (C+B) texture components favored AGG and the bands of $\overline{B}$ texture component were more stable against AGG at the applied PWHT scheme of 60 min ST.

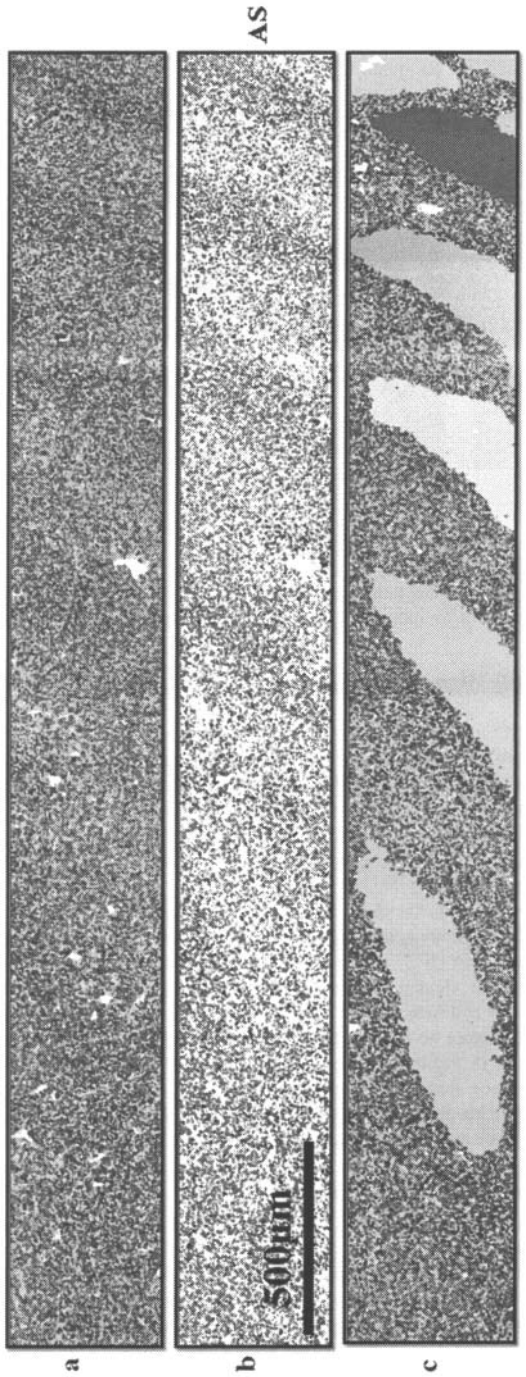

Figure 5, a) EBSD map in IPF colouring relative to ND of AA2017 as FS welded shown in Figure 3, b) Texture component map after rotations with B (red), $\overline{B}$ (yellow), and C (blue) and c) EBSD map in IPF colouring relative to ND of the PWHT AA2017 after FSW for 60min at 500°C. (IPF triangle colouring scale given in Figure 6d)

In terms of texture, Figure 6 shows the calculated 111 and 110 pole figures (PF) for the raw EBSD data set collected from the as FSWed section in (Figure 6a) and from the PWHTed section in (Figure 6b and c). The texture of the as FSWed is dominated by off-axes shear texture as reported before [12, 22-24]. After PWHT the 111 and 110 PFs were calculated for the fine original grains (Figure 6b) and for the large grains (Figure 6c). It can be observed that the original fine grain region retained its off-axes shear texture while the large grains have a random texture.

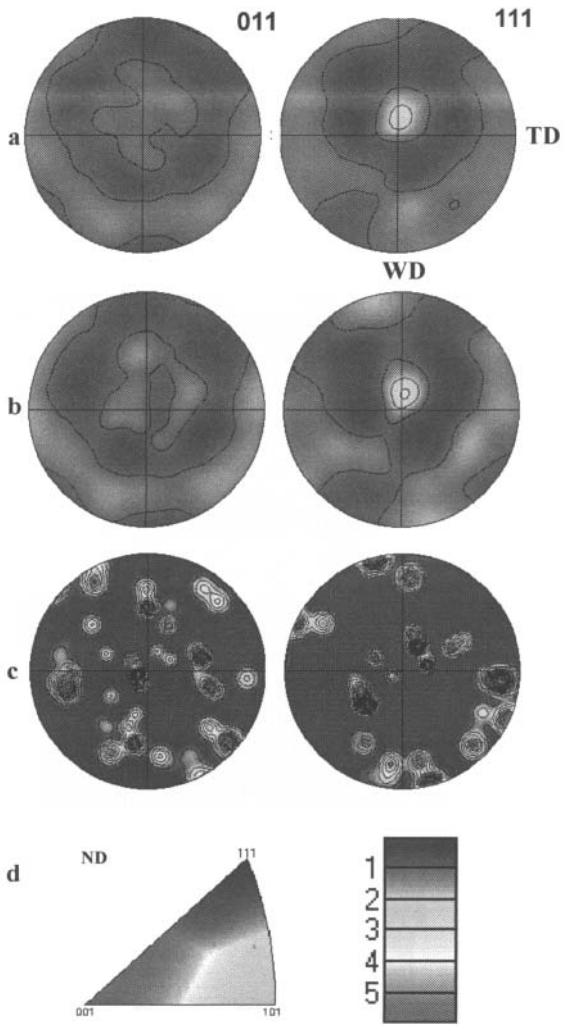

Figure 6, The calculated 111 and 110 PFs from the raw EBSD data set of the as FSWed in (a), of the fine grains in the PWHTed in (b) and of the large grains in the PWHTed in (c). (d) Shows the IPF colouring triangle for EBSD data in Figure 4 and the PF colouring scale.

Conclusions

From the current study it can be concluded that:

1. PWHT of FSWed AA2017 has been resulted in AGG at the bottom of the NG and some areas near the AS, in addition to a very thin layer at the top surface.

2. Grain size of the coarsened area increased by increasing ST time, however the area of grain coarsening almost did not change significantly.

3. PWHT schemes applied could not result in a full hardening of the sections with the hardness increased by increasing ST time.

4. The bands of (C+ B) texture components favored AGG and the bands of $\overline{B}$ texture component were more stable against AGG at the applied PWHT scheme of 60min ST at 500 °C.

Acknowledgment

The authors thank TWI staff of South Yorkshire branch in Sheffield-UK; more especially thank Jonathan Martin of TWI for supplying the weld.

References

1. Chen, Y., H. Liu, and J. Feng, Effect of post-weld heat treatment on the mechanical properties of 2219-O friction stir welded joints,Journal of Materials Science, 2005. 40(17): p. 4657-4659.
2. Chen, Y., H. Liu, and J. Feng, Effect of post-weld heat treatment on the mechanical properties of 2219-O friction stir welded joints, Journal of Materials Science, 2006. 41(1): p. 297-299.
3. Attallah, M.M. and H.G. Salem, Friction stir welding parameters: a tool for controlling abnormal grain growth during subsequent heat treatment, Materials Science and Engineering A, 2005. 391(1-2): p. 51-59.
4. Aydin, H., A. Bayram, and I. Durgun, The effect of post-weld heat treatment on the mechanical properties of 2024-T4 friction stir-welded joints, Materials and Design 2010. 31(5): p. 2568-2577.
5. Elangovan, K. and V. Balasubramanian, Influences of post-weld heat treatment on tensile properties of friction stir-welded AA6061 aluminum alloy joints, Materials Characterization, 2008. 59(9): p. 1168-1177.
6. Ahmed, M.M.Z., B.P. Wynne, W.M. Rainforth, and P.L. Threadgill, An Investigation of Hardness, Microstructure and Crystallographic Texture in Thick Sectioned Friction Stir Welded AA6082,7Th International Friction Stir Welding Symposium, Awaji Island, Japan, 20-22 May, 2008.
7. Karlsen, M., S. Tangen, J. Hjelen, O. Frigaard, and O. Grong. Charactarization of Deformation Microstructure in Friction Stir Welded AA7075 Aluminum Alloy using SEM-EBSD Technique. in 3rd International FSW Symposium, . 2001. Kobe, Japan
8. Charit, I. and R.S. Mishra, Abnormal grain growth in friction stir processed alloys, Scripta Materialia, 2008. 58(5): p. 367-371.
9. Threadgill, P. L., A. J. Leonard, H. R. Shercliff, and P.J. Withers, Friction stir welding of aluminum alloys International Materials Reviews, 2009. 54(2): p. 49-93.
10. Hassan, K.A.A., A.F. Norman, D.A. Price, and P.B. Prangnell, Stability of nugget zone grain structures in high strength Al-alloy friction stir welds during solution treatment, Acta Materialia, 2003. 51(7): p. 1923-1936.
11. Ahmed, M.M.Z., B.P. Wynne, W.M. Rainforth, and P.L. Threadgill, Microstructure, crystallographic texture and mechanical properties of friction stir welded AA2017A,Materials Characterization, 2011. **in revision stage**.
12. Fonda, R.W., J.F. Bingert, and K.J. Colligan. Texture and grain evolutions in a 2195 Friction Stir Weld. in Fifth International Symposium on Friction Stir Welding. 2004. Metz, France.
13. Fonda, R. and J. Bingert, Precipitation and grain refinement in a 2195 Al friction stir weld, Metallurgical and Materials Transactions A, 2006. 37(12): p. 3593-3604.
14. Fonda, R. and J. Bingert, Microstructural evolution in the heat-affected zone of a friction stir weld, Metallurgical and Materials Transactions A, 2004. 35(5): p. 1487-1499.
15. Su, J.Q., T.W. Nelson, R. Mishra, and M. Mahoney, Microstructural investigation of friction stir welded 7050-T651 aluminium, Acta Materialia, 2003. 51(3): p. 713-729.
16. Threadgill, P.L., Terminology in Friction Stir Welding, Science and Technology of Welding and Joining, 2007. 12(4): p. 357-360.
17. Monajati, H., F. Zarandi, M. Jahazi, and S. Yue, Strain induced c0 precipitation in nickel base superalloy Udimet 720 using a stress relaxation based technique, Scripta Materialia, 2005 52: p. 771–776.
18. Pereloma, E.V., B.R. Crawford, and P.D. Hodgson, Strain-induced precipitation behaviour in hot rolled strip steel, Materials Science and Engineering A 2001. 299: p. 27–37.
19. Song, Y., M.D.J. Cross, R.W. M., and W. B.P., Observations of Strain Induced Precipitation during the Thermomechanical Processing of AA6111 Alloy, Materials Science Forum, 2007. 550: p. 211-216.
20. Liu, H.J., Y.C. Chen, and J.C. Feng, Effect of zigzag line on the mechanical properties of friction stir welded joints of an Al-Cu alloy,Scripta Materialia, 2006. 55: p. 231–234.
21. Sato, Y.S., F. Yamashita, Y. Sugiura, S.H.C. Park, and H. Kokawa, FIB-assisted TEM study of an oxide array in the root of a friction stir welded aluminum alloy, Scripta Materialia, 2004. 50(3): p. 365-369.
22. Ahmed, M.M.Z., B.P. Wynne, W.M. Rainforth, and P.L. Threadgill, Quantifying crystallographic texture in the probe-dominated region of thick-section friction-stir-welded aluminum, Scripta Materialia, 2008. 59(5): p. 507-510.
23. Fonda, R.W. and J.F. Bingert, Texture variations in an aluminum friction stir weld, Scripta Materialia, 2007. 57(11): p. 1052-1055.
24. Prangnell, P.B. and C.P. Heason, Grain structure formation during friction stir welding observed by the 'stop action technique', Acta Materialia, 2005. 53(11): p. 3179-3192.